Basic Science

Intracellular Ca^{2+} Transient Phase II Can be Assessed by Half-Logistic Function Model in Isolated Aequorin-Injected Mouse Left Ventricular Papillary Muscle

Ju Mizuno,[1,2,3,4] Mikiya Otsuji,[1] Hideko Arita,[1,3] Kazuo Hanaoka[1,3] and Takeshi Yokoyama[1,4]

Background: Myocardial contraction and relaxation are regulated by increases and decreases in intracellular cytoplasmic calcium (Ca^{2+}) concentration ($[Ca^{2+}]_i$). In previous studies, we found that a half-logistic (h-L) function, which represents a half-curve of a symmetrical sigmoid logistic function with a boundary at the inflection point, curve-fits the first half of the ascending phase (CaTI) and the second half of the descending phase of the $[Ca^{2+}]_i$ transient curve (CaTIV) better than a mono-exponential (m-E) function. In the present study, we investigated the potential application of an h-L function to the analysis of the second half of the ascending phase of the $[Ca^{2+}]_i$ transient curve (CaTII).

Methods: The $[Ca^{2+}]_i$ transient was measured using the Ca^{2+}-sensitive photoprotein aequorin, which was microinjected into 15 isolated left ventricular (LV) papillary muscles of mice. The observed CaTII data during the time duration from the point corresponding to the maximum of the first-order time derivative of Ca^{2+} concentration (dCa/dt_{max}) to the point corresponding to the peak Ca^{2+} concentration was curve-fitted by the least-squares method using the h-L and m-E function equations.

Results: The mean correlation coefficient (r) values of the h-L and m-E curve-fits for CaTII were 0.9996 and 0.9984, respectively. The Z transformation of h-L r was larger than that of m-E r ($p < 0.0001$). H-L residual mean square (RMS) was smaller than m-E RMS ($p < 0.001$).

Conclusions: The h-L function tracks the magnitudes and time courses of CaTII more accurately than the m-E function in isolated aequorin-injected mouse LV papillary muscle. Compared with the m-E time constant, the h-L time constant of CaTII is a more reliable index for evaluating the time duration of the change in the increase in $[Ca^{2+}]_i$ during the combination of the middle part of the contraction process and the early part of the relaxation process. CaTII can be assessed by the h-L function model in cardiac muscles. The h-L approach may provide a more useful model for studying each process in myocardial Ca^{2+} handling.

Key Words: Calcium handling • Calcium transient • Curve-fit • Half-Logistic function • Time constant

Received: March 26, 2012 Accepted: February 6, 2013
[1]Department of Anesthesiology, Faculty of Medicine, The University of Tokyo, Tokyo 113-8549; [2]Department of Anesthesiology and the Intensive Care Unit, Teikyo University School of Medicine, Tokyo 173-8605; [3]Department of Anesthesiology and Pain Relief Center, JR Tokyo General Hospital, Tokyo 151-8528; [4]Department of Dental Anesthesiology, Faculty of Dental Science, Kyushu University, Fukuoka 812-8582, Japan.

Address correspondence and reprint requests to: Dr. Ju Mizuno, Department of Anesthesiology and Intensive Care Unit, Teikyo University School of Medicine, 2-11-1 Kaga, Itabashi-ku, Tokyo 173-8605, Japan. Tel: 81-3-3964-2575; Fax: 81-3-3963-2687; E-mail: mizuno_ju8@yahoo.co.jp

INTRODUCTION

Myocardial contraction and relaxation are regulated by increases and decreases in intracellular cytoplasmic calcium (Ca^{2+}) concentration ($[Ca^{2+}]_i$) in myocardial Ca^{2+} handling and excitation-contraction (E-C) coupling in cardiac muscle cells.[1] The waveforms of the $[Ca^{2+}]_i$ transient provide valuable information for evaluating the change in $[Ca^{2+}]_i$.

Curve-fitting and non-linear regression are valuable

tools for elucidating the mechanism, summarizing information, eliminating noise, allowing speculation regarding unmeasured data, and separating the effects of multiple factors. To maximize the amount of useful information extracted from the $[Ca^{2+}]_i$ transient curve, we previously curve-fitted the first half of the ascending phase of the $[Ca^{2+}]_i$ transient curve (CaTI)[2] and the second half of the descending phase of the $[Ca^{2+}]_i$ transient curve (CaTIV)[3] with a half-logistic (h-L) function, which is a half-curve of a symmetrical sigmoid logistic function with a boundary at the inflection point, better than a mono-exponential (m-E) function. We found that the h-L time constant of the CaTI ($Ca\tau_{1L}$) represents the time duration of the increase in Ca^{2+} concentration from sarcoplasmic reticulum (SR) by Ca^{2+}-induced Ca^{2+} release (CICR) during the early part of the contraction process.[2] Furthermore, we found that the h-L time constant of CaTIV ($Ca\tau_{4L}$) represents the time duration of the decrease in Ca^{2+} concentration resulting from Ca^{2+} sequestration into SR and Ca^{2+} removal from the cytoplasm to the extracellular space through the Na^+/Ca^{2+} exchanger during the late part of the relaxation process.[3] In addition, the second half of the ascending phase of the $[Ca^{2+}]_i$ transient curve (CaTII) probably affects both the middle part of the contraction process and the early part of the relaxation process. We speculated that CaTII can also be represented by the h-L function.

In the present study, we investigated the potential application of the h-L function to the analysis of CaTII in cardiac muscle and sought to determine whether the h-L function curve-fits it more accurately than the m-E function. Improved curve-fit by using the h-L function would provide a reliable time constant and increase our understanding of each process in myocardial Ca^{2+} handling and E-C coupling.

MATERIALS AND METHODS

This study protocol was approved by the Animal Investigation Committee of the Jikei University School of Medicine. All procedures during the experiments were conducted in the Jikei University School of Medicine in conformance with the "Guiding Principles for the Care and Use of Animals in the Field of Physiological Sciences" endorsed by the American Physiological Society and the Physiological Society of Japan.

Surgical preparation

The experimental procedures of our study have been previously described in detail.[2-5] In short, 15 mice (C57BL/6; body weight 25-30 g) were anesthetized with intravenous (1.5-2.0 mg/kg) and intraperitoneal (15-20 mg/kg) pentobarbital sodium, respectively. Following removal of the heart, the aorta was cannulated with a blunted 18 G needle, and the heart was mounted on a Langendorff apparatus. The coronary blood was washed out with Tyrode's solution containing 2 mM Ca^{2+} buffered by *N*-2-hydroxyethyl-piperazine-*N*-2-ethanesulfonic acid (HEPES) at a constant pressure for 5 min. The solution was changed to HEPES-buffered Tyrode's solution containing 2 mM Ca^{2+} and 20 mM 2, 3-butanedione monoxime after the heart beat was stabilized. Once the contraction stopped completely, the heart was removed from the Langendorff apparatus. A thin papillary muscle was dissected out from the mouse left ventricular (LV) walls.

After both ends of the isolated muscle had been tied with silk threads, the muscle was mounted horizontally in an experimental chamber, immersed in a bath and continuously perfused with Tyrode's solution. One end of the muscle was attached to a fixed hook and the other was attached to the arm of a tension transducer (BG-10; Kulite Semiconductor Products, Leonia, NJ, USA; compliance 2.5 μm/g, unloaded resonant frequency 0.6 kHz). A pair of platinum black electrodes was placed parallel to the muscle, which was regularly stimulated by a single square pulse of 5 ms duration and 0.2 Hz; the strength of the stimulation was 1.5-fold the threshold. The muscle was slowly stretched and adjusted to the length at which the developed tension reached maximum (L_{max}).

Aequorin injection

Aequorin was dissolved in 150 mM KCl and 5 mM HEPES, pH 7.0, at a final concentration of 50-100 μM. Using glass micropipettes with a resistance of 30-50 MΩ, we injected aequorin into 150-200 superficial cells of the preparation using nitrogen gas. Aequorin light signals were detected using a photomultiplier (EMI 9789A; Thorn EMI, Ruislip, UK) placed just above the muscle.[6] In twitch response, the aequorin light signal was recorded through a 500-Hz low-pass filter. Sixty-four ae-

quorin light signals were averaged to improve the signal-to-noise ratio.

The measurement of aequorin's light signal was essentially similar to those noted in previous reports.[7,8] Aequorin light signals were converted to $[Ca^{2+}]_i$ using an *in vitro* calibration curve.[9] The constants used in the present experiment were as follows: n, 3.14; K_R, 4,025,000; K_{TR}, 114.6.[10] Ca^{2+} signals were sampled at 1-ms intervals and digitized with an A/D converter. All Ca^{2+} data were stored on tape (NFR-3515W; Sony Magnescale, Tokyo, Japan) and a computer (PC-9801; NEC, Tokyo, Japan) for later analysis.

Tyrode's solution

Tyrode's solution buffered with HEPES was used during all experiments, including muscle dissection and aequorin injection. The composition of the solution (in mM) was as follows: NaCl, 136.9; KCl, 5.4; $MgCl_2$, 0.5; NaH_2PO_4, 0.33; HEPES, 5; glucose, 5. The pH was adjusted to 7.40 ± 0.05 with NaOH at 24 °C, and the solution was equilibrated with 100% O_2. The temperature of the solution was continuously monitored with a thermocouple and maintained at 30 ± 0.5 °C.

Ca^{2+} transients

Ca^{2+} signals were measured from the point before the twitch stimulation procedure was started. The Ca^{2+} signal gradually increased, reached a peak, then decreased and returned to the resting Ca^{2+} concentration before the following twitch stimulation – all within the 1,000-ms sampling window. Signals for CaTII, which extends from the point corresponding to the maximum of the first-order time derivative of Ca^{2+} concentration (dCa/dt_{max}) to the point corresponding to the peak Ca^{2+} concentration, as shown in Figure 1, were used for subsequent analyses. The dCa/dt was obtained by differentiating the sampled Ca^{2+} data after digital smoothening using an 11-point, non-weighted moving average of digitized Ca^{2+} data signals.

h-L function equation

The following h-L function was used to curve-fit CaTII data by the least-squares method as shown in Figure 2A.

$$Ca(t) = 2Ca_{2A}/\{1 + \exp[(t - t_{aC})/Ca\tau_{2L}]\} + Ca_{2B} \qquad \text{(Eq. 1)}$$

where t is the time from the beginning of twitch stimulation to the point corresponding to the Ca^{2+} concentration, Ca_{2A} is the h-L amplitude constant of CaTII, $Ca\tau_{2L}$ is the h-L time constant of CaTII, Ca_{2B} is the h-L non-zero asymptote of CaTII, and t_{aC} is a constant which represents the time at the point corresponding to dCa/dt_{max}. It is noted that t_{aC} is determined before the h-L curve fitting. The h-L function curve given by Eq. 1 increases monotonically from $Ca(t_{aC})$ [= $(Ca_{2A} + Ca_{2B})$] to $Ca(\infty)$ [= Ca_{2B}]. $Ca\tau_{2L}$ value corresponds to the time duration for the curves to increase from $Ca(t_{aC})$ [= $(Ca_{2A} + Ca_{2B})$] to $Ca(t_{aC} + Ca\tau_{2L})$ {= $[2Ca_{2A}/(1 + e) + Ca_{2B}]$~$(0.54\ Ca_{2A} + Ca_{2B})$}.

M-E function equation

An m-E function was also used to curve-fit CaTII data by the least-squares method as shown in Figure 2B.

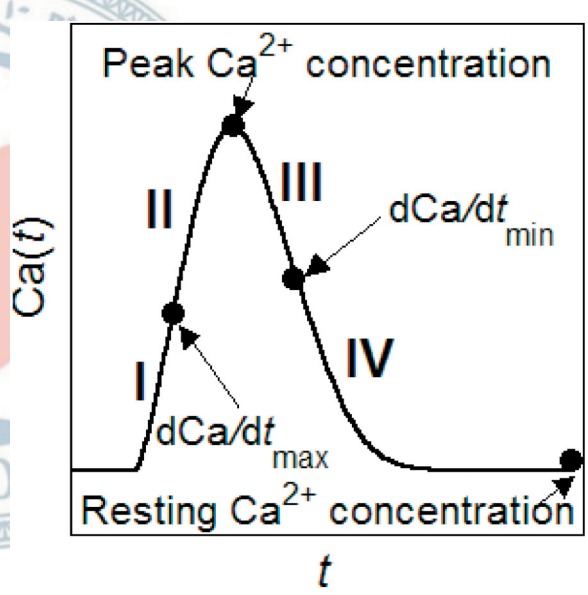

Figure 1. *$[Ca^{2+}]_i$ transient curve schema. The $[Ca^{2+}]_i$ transient curve is divided into four sequential phases. The first half of the ascending phase of the $[Ca^{2+}]_i$ transient curve (CaTI) is the curve from the point corresponding to the beginning of twitch stimulation to the point corresponding to the maximum of the first-order time derivative of Ca^{2+} concentration (dCa/dt_{max}). The second half of the ascending phase of the $[Ca^{2+}]_i$ transient curve (CaTII) is the curve from the point corresponding to dCa/dt_{max} to the point corresponding to the peak Ca^{2+} concentration. The first half of the descending phase of the $[Ca^{2+}]_i$ transient curve (CaTIII) is the curve from the point corresponding to the peak Ca^{2+} concentration to the point corresponding to the minimum of the first-order time derivative of Ca^{2+} concentration (dCa/dt_{min}). The second half of the descending phase of the $[Ca^{2+}]_i$ transient curve (CaTIV) is the curve from the point corresponding to dCa/dt_{min} to the point corresponding to the resting Ca^{2+} concentration.*

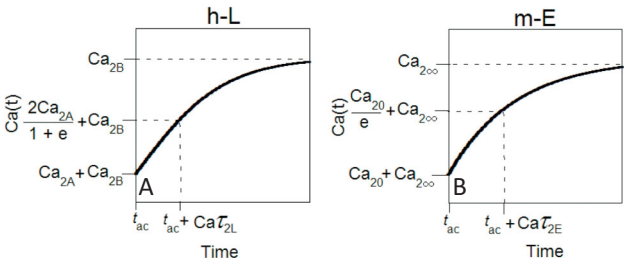

Figure 2. *Half-logistic (h-L) and mono-exponential (m-E) distribution function curves for the second half of the ascending phase of the $[Ca^{2+}]_i$ transient curve (CaTII). (A) The h-L function curve described in Equation 1 (see text). Ca_{2A}, h-L amplitude constant of CaTII; $Ca\tau_{2L}$, h-L time constant of CaTII; Ca_{2B}, h-L non-zero asymptote of CaTII; t_{aC}, time at the point corresponding to the maximum of the first-order time derivative of Ca^{2+} concentration (dCa/dt_{max}). (B) The m-E function curve described in Equation 2. Ca_{20}, m-E amplitude constant of CaTII; $Ca\tau_{2E}$, m-E time constant of CaTII; $Ca_{2\infty}$, m-E non-zero asymptote of CaTII.*

$$Ca(t) = Ca_{20}\exp[-(t - t_{aC})/Ca\tau_{2E}] + Ca_{2\infty} \quad \text{(Eq. 2)}$$

where t is the time from the beginning of twitch stimulation to the point corresponding to the Ca^{2+} concentration, Ca_{20} is the m-E amplitude constant of CaTII, $Ca\tau_{2E}$ is the m-E time constant of CaTII, $Ca_{2\infty}$ is the m-E non-zero asymptote of CaTII, and t_{aC} is a constant which represents the time at the point corresponding to dCa/dt_{max}. It is noted that t_{aC} is determined before the m-E curve fitting. The m-E function curve given by Eq. 2 increases monotonically from $Ca(t_{aC})$ [= $(Ca_{20} + Ca_{2\infty})$] to $Ca(\infty)$ [= $Ca_{2\infty}$]. The $Ca\tau_{2E}$ value corresponds to the time duration for the curve to increase from $Ca(t_{aC})$ [= $(Ca_{20} + Ca_{2\infty})$] to $Ca(t_{aC} + Ca\tau_{2E})$ [= $(Ca_{20}/e + Ca_{2\infty}) \sim (0.37\ Ca_{20} + Ca_{2\infty})$].

It should be noted that the h-L function (Eq. 1) has the same number (three) of variable parameters as the m-E function (Eq. 2) and that Ca_{2A}, $Ca\tau_{2L}$, and Ca_{2B} in Eq. 1 are conceptually similar to Ca_{20}, $Ca\tau_{2E}$, and $Ca_{2\infty}$ in Eq. 2, respectively.

Statistical analysis

Goodness of fit was evaluated with the correlation coefficient (r) and residual mean square (RMS) for the h-L and m-E curve-fitting models. Fisher's Z transformation (Z) of r [11] was calculated with the following equation: $Z = 1/2[\ln(1 + r) - \ln(1 - r)]$. Residual values were calculated as the observed CaTII data minus the best-fit h-L or m-E value at each sampling data point. RMS was calculated as the residual sum of squares (RSS) divided by the residual degrees of freedom, which indicates the number of data points analyzed minus the number of parameters in the function.[12]

Analyses were performed using Statcel (OMS, Saitama, Japan), StatView ver 5.0 (SAS Institute, Cary, NC, USA), and Deltagraph 5.4.5v J (Deltapoint, Monterey, CA, USA) software. Values in the text are expressed as the mean ± standard deviation (SD) unless otherwise noted. The Z of r and RMS values were compared between the goodness of h-L and m-E fits. The Student's paired t test was used for comparison between h-L and m-E Z and Wilcoxon signed-rank test was used for comparison between h-L and m-E RMS. Simple linear regression analyses were performed between the amplitude constants and between the time constants for the different $[Ca^{2+}]_i$ transient phases. A p value of < 0.05 was considered to indicate statistical significance.

RESULTS

Measurements of Ca^{2+} transient

The muscle length and diameter of the 15 isolated aequorin-injected LV papillary muscle specimens of mice were 2.01 ± 0.43 and 0.63 ± 0.11 mm, respectively.

Table 1 summarizes the representative values from the entire magnitude and time course of $[Ca^{2+}]_i$ transient data. The time duration from the point corresponding to dCa/dt_{max} up to the point corresponding to the peak Ca^{2+} concentration, which corresponds to CaTII, was 16.5 ± 1.6 ms.

Table 1. Observed values of the $[Ca^{2+}]_i$ transient curve

Observed value	
Ca^{2+} concentration at dCa/dt_{max} (nmol/l)	819 ± 189
Peak Ca^{2+} concentration (nmol/l)	$1,694 \pm 384$
Ca^{2+} concentration at dCa/dt_{min} (nmol/l)	$1,259 \pm 440$
Time to dCa/dt_{max} (ms)	60.1 ± 1.4
Time to peak Ca^{2+} concentration (ms)	76.1 ± 2.1
Time to dCa/dt_{min} (ms)	106.4 ± 14.9
dCa/dt_{max} (nmol/l/ms)	119.8 ± 28.7
dCa/dt_{min} (nmol/l/ms)	$-20.9. \pm 4.6$

Data are presented as the mean ± standard deviation of the observed values of the $[Ca^{2+}]_i$ transient curves in the 15 isolated aequorin-injected left ventricular papillary muscles of mice. dCa/dt_{max}, maximum of the first-order time derivative of Ca^{2+} concentration; dCa/dt_{min}, minimum of the first-order time derivative of Ca^{2+} concentration.

H-L and m-E curve-fits

The representative best-fitted h-L and m-E function curves for the observed CaTII data in the muscle of a mouse are shown in Figures 3A and B, respectively. The residual Ca^{2+} concentrations calculated from the observed CaTII data minus the best-fitted h-L and m-E curves are shown in Figures 3C and D, respectively.

The h-L and m-E function parameters for CaTII in the 15 specimens are shown in Table 2.

Goodness of h-L and m-E fits

The mean *r* value of the h-L and m-E curve-fitted for CaTII in the 15 specimens was 0.9996 and 0.9984, respectively. The *Z* transformation value of the h-L and m-E *r* was 4.31 ± 0.93 and 3.57 ± 0.35, respectively. H-L *Z* was significantly larger than m-E *Z* ($p < 0.0001$).

The h-L and m-E RMS values were 106 ± 172 and 416 ± 433 $(nmol/l)^2$, respectively. H-L RMS was significantly smaller than m-E RMS ($p < 0.001$).

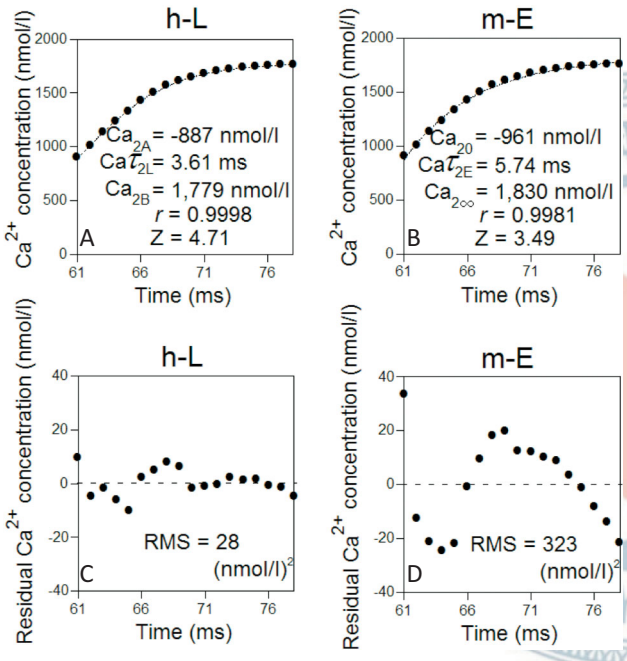

Figure 3. *Representative best-fitted half-logistic (h-L) and mono-exponential (m-E) function curves for the observed second half of the ascending phase of the $[Ca^{2+}]_i$ transient curve (CaTII) data during the time duration from the point corresponding to the maximum of the first-order time derivative of Ca^{2+} concentration (dCa/dt_{max}) to the point corresponding to the peak Ca^{2+} concentration in the isolated aequorin-injected left ventricular papillary muscle of a mouse. (A) Representative best-fitted h-L function curve (thin dotted line) for the observed CaTII data (black dots). Ca_{2A}, h-L amplitude constant of CaTII; $Ca\tau_{2L}$, h-L time constant of CaTII; Ca_{2B}, h-L non-zero asymptote of CaTII; r, correlation coefficient; Z, Z transformation of r. (B) Representative best-fitted m-E function curve (thin dotted line) for the observed CaTII data (black dots). Ca_{20}, m-E amplitude constant of CaTII; $Ca\tau_{2E}$, m-E time constant of CaTII; $Ca_{2\infty}$, m-E non-zero asymptote of CaTII. (C) Residual Ca^{2+} concentrations calculated from the observed CaTII data minus the best-fitted h-L curve. RMS, residual mean square. (D) Residual Ca^{2+} concentrations calculated from the observed CaTII data minus the best-fitted m-E curve.*

DISCUSSION

These results demonstrate that the h-L function curve-fits CaTII more accurately than the m-E function in isolated aequorin-injected LV papillary muscle of mice. Therefore, we suggest that the h-L function model can be used to more reliably characterize the magnitude and time course of CaTII in cardiac muscle.

Ca^{2+} handling

During a cardiac cycle, the contraction process causes Ca^{2+} inflow into the cytoplasm through voltage-dependent sarcolemmal L-type Ca^{2+} channels and release of Ca^{2+} from SR induced by Ca^{2+} influx through sarcolemmal L-type Ca^{2+} channels[13,14] and the sensitivity of myofilaments to Ca^{2+}. Most Ca^{2+} flows into the cytoplasm from SR by CICR, with only a small amount of Ca^{2+} flowing into the cytoplasm through L-type Ca^{2+} channels. During each heart beat, a transient increase in the myocardial $[Ca^{2+}]_i$ induces a transient increase in the binding of Ca^{2+} to a major Ca^{2+}-binding protein, troponin C (TnC), and a transient increase in attachment of the thick filament myosin cross-bridge to thin filament

Table 2. Calculated half-logistic (h-L) and mono-exponential (m-E) function parameters for the second half of the ascending phase of the $[Ca^{2+}]_i$ transient curve (CaTII)

h-L		m-E	
Ca_{2A}	-914 ± 249 nmol/l	Ca_{20}	-997 ± 274 nmol/l
$Ca\tau_{2L}$	3.75 ± 0.46 ms	$Ca\tau_{2E}$	6.06 ± 0.85 ms
Ca_{2B}	1,730 ± 395 nmol/l	$Ca_{2\infty}$	1,790 ± 410 nmol/l

Data are presented as the mean ± standard deviation of the calculated values of the h-L and m-E function parameters for CaTII in the 15 isolated aequorin-injected left ventricular papillary muscles of mice. Ca_{2A}, h-L amplitude constant of CaTII; $Ca\tau_{2L}$, h-L time constant of CaTII; Ca_{2B}, h-L non-zero asymptote of CaTII; Ca_{20}, m-E amplitude constant of CaTII; $Ca\tau_{2E}$, m-E time constant of CaTII; $Ca_{2\infty}$, m-E non-zero asymptote of CaTII.

actin, which precedes and initiates myocardial contraction and increase in LV pressure. Because myocardial contraction lags behind the change in $[Ca^{2+}]_i$, the magnitude of the contraction is determined not only by the magnitude of $[Ca^{2+}]_i$ but also by its time duration. The relaxation process involves Ca^{2+} dissociation from TnC, Ca^{2+} sequestration into SR,[15] and Ca^{2+} removal from the cytoplasm to the extracellular space through the Na^+/Ca^{2+} exchanger.[16]

Waveform analysis

The $[Ca^{2+}]_i$ transient curve is expected to change in tandem with the magnitudes and time courses of the myocardial tension and LV pressure curves. We have reported that the h-L function outperforms m-E function in curve-fitting the following: (i) the second half of the ascending phase of the isometric myocardial tension curve during the time duration from the point corresponding to the maximum of the first-order time derivative of tension (dF/dt_{max}) to the point corresponding to the peak tension in the myocardial muscle[4] and (ii) the second half of the ascending phase of the isovolumic LV pressure curve during the time duration from the point corresponding to the maximum of the first-order time derivative of LV pressure (dP/dt_{max}) to the point corresponding to the peak LV pressure in the cross-circulated dog heart.[17]

The calculated function parameters were used to summarize the waveform of each $[Ca^{2+}]_i$ transient phase with almost no loss of information on the characteristics. The m-E function has been used for curve-fitting CaTI shown in Figure 1, in the papillary muscles of mice[2] and rabbits,[2] and CaTIV shown in Figure 1, in the isovolumic LV in excised whole hearts of rats,[18-20] and in myocytes of mice,[3,21,22] rabbits,[3,22,23] rats,[23-25] dogs[22] and humans.[22] For example, there are significant differences in the m-E time constant of CaTIV ($Ca\tau_{4E}$), reflecting activities of the SR Ca^{2+}-ATPase, with values for myocytes of humans > dogs > rabbits > mice.[22] In previous and present studies, we found that reliable CaTI,[2] CaTII, and CaTIV[3] can be predicted from the best-fitted h-L function curves.

Magnitude of $[Ca^{2+}]_i$ transient phase

The calculated Ca_{2A} and Ca_{2B} have physiological and mathematical meanings. The absolute value of Ca_{2A} represents the difference between Ca^{2+} concentration at the point corresponding to the maximum rate of increase in the cytoplasmic Ca^{2+} concentration, i.e., dCa/dt_{max}, and the peak Ca^{2+} concentration, as shown in Figure 2A. Ca_{2B} represents Ca^{2+} concentration at the point corresponding to the peak Ca^{2+} concentration.

There were significant relationships between the h-L amplitude constant of CaTI (Ca_{1A}) and the absolute value of Ca_{2A}, as shown in Figure 4A, and between the m-E amplitude constant of CaTI (Ca_{10}) and the absolute value of Ca_{20}, as shown in Figure 4B (see APPENDIX). Similarly, there were significant relationships between the h-L amplitude constant of CaTIV (Ca_{4A}) and the absolute value of Ca_{2A}, as shown in Figure 4C, and between the m-E amplitude constant of CaTIV (Ca_{40}) and the absolute value of Ca_{20}, as shown in Figure 4D. These results show that the magnitude of CaTII relates to that of CaTI and CaTII. Therefore, the proportion of the magnitude of CaTII to CaTI and that of CaTII to CaTIV is constant.

Time constant of $[Ca^{2+}]_i$ transient phase

The time constant for each $[Ca^{2+}]_i$ transient phase is used for comparison of the time duration. The h-L time constant of CaTI ($Ca\tau_{1L}$) represents the time duration from the point where $Ca = 2Ca_{1A}/(1+e) + Ca_{1B}$ to the point where $Ca = Ca_{1A} + Ca_{1B}$[2] (see APPENDIX). The h-L time constant of CaTIV ($Ca\tau_{4L}$) represents the time duration from the point where $Ca = Ca_{4A} + Ca_{4B}$ to the point where $Ca = 2Ca_{4A}/(1+e) + Ca_{4B}$.[3] The m-E time constant of CaTI ($Ca\tau_{1E}$) represents the time duration from the point where $Ca = Ca_{10}/e + Ca_{1\infty}$ to the point where $Ca = Ca_{10} + Ca_{1\infty}$[2] and $Ca\tau_{4E}$ represents the time duration from the point where $Ca = Ca_{40} + Ca_{4\infty}$ to the point where $Ca = Ca_{40}/e + Ca_{4\infty}$.[3] From statistical analyses, $Ca\tau_{1L}$ and $Ca\tau_{4L}$ are more reliable indices of the time durations of the changes in the increase and decrease in $[Ca^{2+}]_i$ than $Ca\tau_{1E}$ and $Ca\tau_{4E}$, respectively.[2,3] In the present study, compared with $Ca\tau_{2E}$, $Ca\tau_{2L}$ is also a more reliable index of the time duration of the change in $[Ca^{2+}]_I$ during CaTII.

There were no significant relationships between $Ca\tau_{1L}$ and $Ca\tau_{2L}$, as shown in Figure 5A, and between $Ca\tau_{1E}$ and $Ca\tau_{2E}$, as shown in Figure 5B. $Ca\tau_{2L}$ and $Ca\tau_{2E}$ were significantly larger than $Ca\tau_{1L}$ and $Ca\tau_{1E}$, respectively, tested using Student's paired *t* test ($p < 0.0001$).

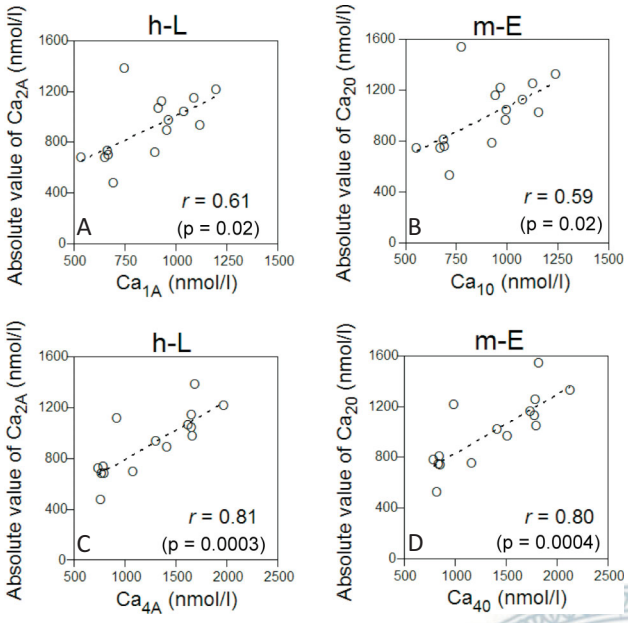

Figure 4. *Relationship between the amplitudes best-fitted for the first half of the ascending phase of the $[Ca^{2+}]_i$ transient curve (CaTI) data and for the second half of the ascending phase of the $[Ca^{2+}]_i$ transient curve (CaTII) data as well as the relationship between the amplitudes best-fitted for the second half of the descending phase of the $[Ca^{2+}]_i$ transient curve (CaTIV) data and for the CaTII data in the 15 isolated aequorin-injected left ventricular (LV) papillary muscles of mice. (A) Points of intersection (open circles) between the half-logistic (h-L) amplitude constant of the CaTI data during the time duration from the point corresponding to the beginning of twitch stimulation to the point corresponding to the maximum of the first-order time derivative of Ca^{2+} concentration (dCa/dt_{max}) (Ca_{1A}) and the absolute values of the h-L amplitude constant of the CaTII data (Ca_{2A}). (B) Points of intersection (open circles) between the mono-exponential (m-E) amplitude constant of the CaTI data (Ca_{10}) and the absolute values of the m-E amplitude constant of the CaTII data (Ca_{20}). (C) Points of intersection (open circles) between the h-L amplitude constant of the CaTIV data during the time duration from the point corresponding to the minimum of the first-order time derivative of Ca^{2+} concentration (dCa/dt_{min}) to the point corresponding to the resting Ca^{2+} concentration (Ca_{4A}) and the absolute values of Ca_{2A}. (D) Points of intersection (open circles) between the m-E amplitude constant of the CaTIV data (Ca_{40}) and the absolute values of Ca_{20}. r, correlation coefficient.*

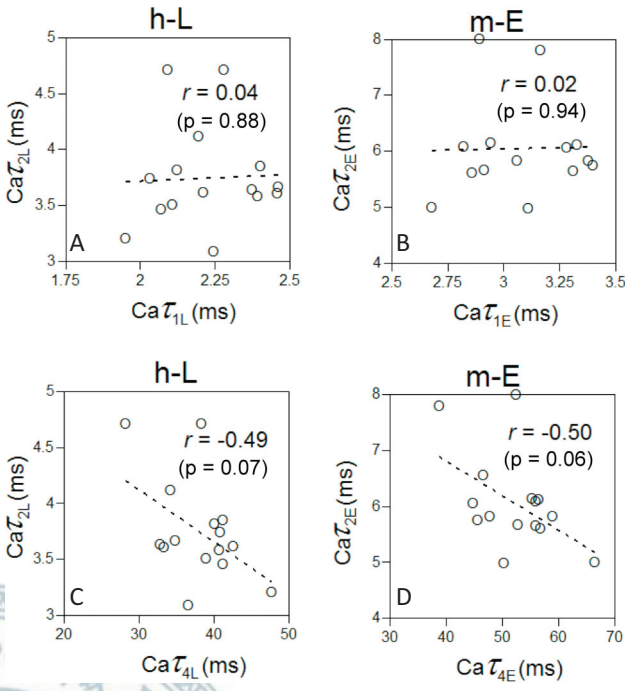

Figure 5. *Relationship between the time constants best-fitted for the first half of the ascending phase of the $[Ca^{2+}]_i$ transient curve (CaTI) data and for the second half of the ascending phase of the $[Ca^{2+}]_i$ transient curve (CaTII) data as well as the relationship between the time constants best-fitted for the second half of the descending phase of the $[Ca^{2+}]_i$ transient curve (CaTIV) data and for the CaTII data in the 15 isolated aequorin-injected left ventricular (LV) papillary muscles of mice. (A) Points of intersection (open circles) between the half-logistic (h-L) time constant of the CaTI data during the time duration from the point corresponding to the beginning of twitch stimulation to the point corresponding to the maximum of the first-order time derivative of Ca^{2+} concentration (dCa/dt_{max}) ($Ca\tau_{1L}$) and the h-L time constant of the CaTII data ($Ca\tau_{2L}$). (B) Points of intersection (open circles) between the mono-exponential (m-E) time constant of the CaTI data ($Ca\tau_{1E}$) and the m-E time constant of the CaTII data ($Ca\tau_{2E}$). (C) Points of intersection (open circles) between the h-L time constant of the CaTIV data during the time duration from the point corresponding to the minimum of the first-order time derivative of Ca^{2+} concentration (dCa/dt_{min}) to the point corresponding to the resting Ca^{2+} concentration ($Ca\tau_{4L}$) and $Ca\tau_{2L}$. (D) Points of intersection (open circles) between the m-E time constant of the CaTIV data ($Ca\tau_{4E}$) and $Ca\tau_{2E}$. r, correlation coefficient.*

Similarly, there were no significant relationships between $Ca\tau_{4L}$ and $Ca\tau_{2L}$, as shown in Figure 5C, and between $Ca\tau_{4E}$ and $Ca\tau_{2E}$, as shown in Figure 5D. $Ca\tau_{2L}$ and $Ca\tau_{2E}$ were significantly smaller than $Ca\tau_{4L}$ and $Ca\tau_{4E}$ ($p < 0.0001$), respectively. $Ca\tau_{2L}$ is independent of $Ca\tau_{1L}$ and $Ca\tau_{4L}$. Taken together, these data indicate that the time change in $[Ca^{2+}]_i$ of CaTII is different from that of CaTI and CaIV. Therefore, these results indicate that each $[Ca^{2+}]_i$ transient phase has its own time constant, and there may be individual differences in Ca^{2+} handling such as Ca^{2+} flow into the cytoplasm from SR by CICR during the contraction process, Ca^{2+} sequestration into SR, and Ca^{2+} removal from the cytoplasm to the extracellular space through the Na^+/Ca^{2+} exchanger during the relaxation process in isolated papillary muscle.

CaTI encompasses the beginning phase of the increase in Ca^{2+} concentration from SR by CICR in myocardial Ca^{2+} handling, where $Ca\tau_{1L}$ evaluates the time duration of the change in the increase in $[Ca^{2+}]_i$ during the

early part of the contraction process.[2] On the other hand, CaTIV refers to the ending phase of the decrease in Ca^{2+} concentration by Ca^{2+} sequestration into SR and Ca^{2+} removal from the cytoplasm to the extracellular space through the Na^+/Ca^{2+} exchanger in myocardial Ca^{2+} handling. $Ca\tau_{4L}$ evaluates the time duration of the change in the decrease in $[Ca^{2+}]_i$ during the last part of the relaxation process.[3] CaTII corresponds to the combination of the holding phase of the increase in Ca^{2+} concentration from SR by CICR and the beginning phase of the decrease in Ca^{2+} concentration by Ca^{2+} sequestration into SR and Ca^{2+} removal from the cytoplasm to the extracellular space through the Na^+/Ca^{2+} exchanger.[5] Furthermore, CaTII includes both the middle part of the contraction process and the early part of the relaxation process and represents the change in the difference between the increase and decrease in Ca^{2+} concentration, although the degree of increase in Ca^{2+} concentration is larger than that of decrease in Ca^{2+} concentration. Accordingly, $Ca\tau_{2L}$ evaluates the time duration of the change in the increase in $[Ca^{2+}]_i$ during the combination of the middle part of the contraction process and the early part of the relaxation process. As can be seen in Figures 5C and D, there was a tendency of a slight negative correlation between the time constants of CaTII and CaTIV. We suggest that the change in $[Ca^{2+}]_i$ of CaTII with the contraction and relaxation processes relates to the change in $[Ca^{2+}]_i$ of CaTIV with the simple relaxation process. It may be possible to obtain significant insight into each process in myocardial Ca^{2+} handling and E-C coupling by using $Ca\tau_{1L}$, $Ca\tau_{2L}$, and $Ca\tau_{4L}$.

The calculated h-L function parameters can enable the comparison between the magnitudes and time constants of the observed CaTII. Curve-fitting for the observed CaTI, CaTII, and CaTIV by the h-L function would be useful for studying the effect of $[Ca^{2+}]_i$ during each process in the myocardial Ca^{2+} handling.

Sigmoid logistic function model

The logistic function has been widely used to study rising phenomena in many fields of bioscience and to intuitively describe symmetrical sigmoid curves whose inflection point corresponds to a boundary, such as those found in mortality data[26] and growth curves.[27,28] The logistic nature of these phenomena predicts that the process is initially minimal, increases gradually, and maximizes to an upper asymptote: conversely, is initially maximal, decreases gradually, and minimizes to a lower asymptote. The logistic function is limited in its ability to represent the symmetrical sigmoid function, especially as it reaches the upper or lower asymptote. In a previous study, we reported that the sigmoid logistic function satisfactorily curve-fits well the entire ascending phase during the time duration from the point corresponding to the beginning of twitch stimulation to the point corresponding to the peak Ca^{2+} concentration and the entire descending phase during the time duration from the point corresponding to the peak Ca^{2+} concentration to the point corresponding to the resting Ca^{2+} concentration.[5] Computer simulation of the $[Ca^{2+}]_i$ transient also provided a characterization of the sigmoid logistic function.[29]

Curve-fitting for the entire ascending phase of the $[Ca^{2+}]_i$ transient data by the sigmoid logistic function would be useful for evaluating dCa/dt_{max}. In the present study, however, we found that the entire ascending phase of the $[Ca^{2+}]_i$ transient curve is asymmetrical at the point corresponding to dCa/dt_{max}. SDs of $Ca\tau_{2L}$ and $Ca\tau_{2E}$ were larger than those of $Ca\tau_{1L}$ and $Ca\tau_{1E}$. The asymptote of CaTII, i.e., $dCa/dt = 0$, is only one point, and CaTI has a longer asymptote.

Study limitations

There are several limitations of this study. First, the experimental condition used to measure the $[Ca^{2+}]_i$ transient was not physiological, i.e., 100% L_{max} with 2 mM extracellular Ca^{2+} at 30 °C and a stimulation frequency of 0.2 Hz. Further examination of these concepts is needed under different physiological conditions of preloads, Ca^{2+} concentrations, temperatures, stimulation frequencies, and pharmacological conditions with varying degrees of blocking or stimulating agents of channels, pumps, exchangers, α- and β-adrenergic receptors, and anesthetic agents. Moreover, it will be beneficial if the future studies include a pathological model, such as dilated cardiomyopathy, hypertrophic cardiomyopathy, and ischemic heart failure to demonstrate correlations of h-L function parameters with changes in Ca^{2+} regulation proteins. Second, we used the Ca^{2+}-sensitive photoprotein aequorin, which is a good indicator of the change in $[Ca^{2+}]_i$. Additional investigations with other Ca^{2+}-sensitive fluorescent indicators, such as indo-1, rhod-2, fura-2, and fluo-3, would

be useful. Third, we curve-fitted CaTII using the h-L function model with three variable parameters, i.e., amplitude constant, time constant, and non-zero asymptote. We intend to develop the h-L function with an additional variable parameter or a new function to curve-fit it more accurately.

The first half of the descending phase of the $[Ca^{2+}]_i$ transient curve (CaTIII) shown in Figure 1 corresponds to the combination of the ending phase of the increase in Ca^{2+} concentration from SR by CICR and the holding phase of the decrease in Ca^{2+} concentration by Ca^{2+} sequestration into SR and Ca^{2+} removal from the cytoplasm to the extracellular space through the Na^+/Ca^{2+} exchanger.[5] Moreover, CaTIII also encompasses both the last part of the contraction process and the middle part of the relaxation process and represents the change in the difference between the increase and decrease in $[Ca^{2+}]_i$, although the degree of decrease in $[Ca^{2+}]_i$ is larger than that of increase in $[Ca^{2+}]_i$. The h-L time constant of CaTIII ($Ca\tau_{3L}$) evaluates the time duration of the change in the decrease in $[Ca^{2+}]_i$ during the combination of the last part of the contraction process and the middle part of the relaxation process. However, CaTIII may not be curve-fitted by h-L and m-E functions. Because CaTIII may be straight rather than convex, the inflexion point of the entire descending phase could not be identified. Further examination is needed to determine the location of the inflexion point of the entire descending phase.

CONCLUSIONS

The h-L functions can describe the magnitudes and time courses of not only CaTI and CaTIV but also CaTII more accurately than the m-E functions in isolated aequorin-injected mouse LV papillary muscle. Compared with $Ca\tau_{2E}$, $Ca\tau_{2L}$ is a more reliable index for evaluating the time duration of the change in the increase in $[Ca^{2+}]_i$ during the combination of the middle part of the contraction process and the early part of the relaxation process. CaTII can be assessed by the h-L function model in cardiac muscles. The time constant of CaTII is independent of that of CaTI and CaTIV, although the magnitude of CaTII relates to that of CaTI and CaTIV. The h-L approach may provide a more useful model for studying individual processes in myocardial Ca^{2+} handling.

ACKNOWLEDGEMENTS

We would like to thank Drs. Shuta Hirano, Yoichiro Kusakari, and Satoshi Kurihara at the Department of Cell Physiology, The Jikei University School of Medicine, for their excellent research assistance.

REFERENCES

1. Kurihara S. Regulation of cardiac muscle contraction by intracellular Ca^{2+}. *Jpn J Physiol* 1994;44:591-611.
2. Mizuno J, Hanaoka K, Otsuji M, et al. Calcium-induced calcium release from the sarcoplasmic reticulum can be evaluated with a half-logistic function model in aequorin-injected cardiac muscles. *J Anesth* 2011;25:831-8.
3. Mizuno J, Otsuji M, Takeda K, et al. Superior logistic model for decay of Ca^{2+} transient and isometric relaxation force curve in rabbit and mouse papillary muscles. *Int Heart J* 2007;48:215-32.
4. Mizuno J, Morita S, Otsuji M, et al. Half-logistic time constants as inotropic and lusitropic indices for four sequential phases of isometric tension curves in isolated rabbit and mouse papillary muscles. *Int Heart J* 2009;50:389-404.
5. Mizuno J, Otsuji M, Arita H, et al. Characterization of intracellular Ca^{2+} transient by the hybrid logistic function in aequorin-injected rabbit and mouse papillary muscles. *J Physiol Sci* 2007;57:349-59.
6. Allen DG, Kurihara S. The effects of muscle length on intracellular calcium transients in mammalian cardiac muscle. *J Physiol* 1982;327:79-94.
7. Hirano S, Kusakari Y, O-Uchi J, et al. Intracellular mechanism of the negative inotropic effect induced by α1-adrenoceptor stimulation in mouse myocardium. *J Physiol Sci* 2006;56:297-304.
8. Ishikawa T, Mochizuki S, Kurihara S. Cross-bridge-dependent change of the Ca^{2+} sensitivity during relaxation in aequorin-injected tetanized ferret papillary muscles. *Circ J* 2006;70:913-8.
9. Allen DG, Blinks JR, Prendergast FG. Aequorin luminescence: relation of light emission to calcium concentration-a calcium-independent component. *Science* 1977;195:996-8.
10. Okazaki O, Suda N, Hongo K, et al. Modulation of Ca^{2+} transients and contractile properties by β-adrenoceptor stimulation in ferret ventricular muscles. *J Physiol* 1990;423:221-40.
11. Snedecor GW, Cochran WG. *Statistical methods*. 6th ed. Ames: Iowa State University Press, 1971:185.
12. Thompson DS, Waldron CB, Coltart DJ, et al. Estimation of time constant of left ventricular relaxation. *Br Heart J* 1983;49:250-8.
13. Fabiato A. Time and calcium dependence of activation and inactivation of calcium-induced release of calcium from the sarcoplasmic reticulum of a skinned canine cardiac Purkinje cell. *J Gen Physiol* 1985;85:247-89.
14. Beuckelmann DJ, Wier WG. Mechanism of release of calcium

from sarcoplasmic reticulum of guinea-pig cardiac cells. *J Physiol* 1988;405:233-55.
15. Frank KF, Bölck B, Brixius K, et al. Modulation of SERCA: implications for the failing human heart. *Basic Res Cardiol* 2002;97 Suppl 1:I72-8.
16. Chen S, Li S. The Na^+/Ca^{2+} exchanger in cardiac ischemia/reperfusion injury. *Med Sci Monit* 2012;18:RA161-5.
17. Mizuno J, Shimizu J, Mohri S, et al. Hypovolemia does not affect speed of isovolumic left ventricular contraction and relaxation in excised canine heart. *Shock* 2008;29:395-401.
18. Camacho SA, Brandes R, Figueredo VM, et al. Ca^{2+} transient decline and myocardial relaxation are slowed during low flow ischemia in rat hearts. *J Clin Invest* 1994;93:951-7.
19. Chang KC, Schreur JH, Weiner MW, et al. Impaired Ca^{2+} handling is an early manifestation of pressure-overload hypertrophy in rat hearts. *Am J Physiol* 1996;271:H228-34.
20. Halow JM, Figueredo VM, Shames DM, et al. Role of slowed Ca^{2+} transient decline in slowed relaxation during myocardial ischemia. *J Mol Cell Cardiol* 1999;31:1739-48.
21. Lim CC, Apstein CS, Colucci WS, et al. Impaired cell shortening and relengthening with increased pacing frequency are intrinsic to the senescent mouse cardiomyocyte. *J Mol Cell Cardiol* 2000;32:2075-82.
22. Su Z, Li F, Spitzer KW, et al. Comparison of sarcoplasmic reticulum Ca^{2+}-ATPase function in human, dog, rabbit, and mouse ventricular myocytes. *J Mol Cell Cardiol* 2003;35:761-7.
23. Bassani JWM, Bassani RA, Bers DM. Relaxation in rabbit and rat cardiac cells: species-dependent differences in cellular mechanisms. *J Physiol* 1994;476:279-93.
24. Bers DM, Berlin JR. Kinetics of $[Ca]_i$ decline in cardiac myocytes depend on peak $[Ca]_i$. *Am J Physiol* 1995;268:C271-7.
25. Brittsan AG, Ginsburg KS, Chu G, et al. Chronic SR Ca^{2+}-ATPase inhibition causes adaptive changes in cellular Ca^{2+} transport. *Circ Res* 2003;92:769-76.
26. Wilson DL. The analysis of survival (mortality) data: fitting Gompertz, Weibull, and logistic functions. *Mech Ageing Dev* 1994; 74:15-33.
27. Sheehy JE, Mitchell PL, Ferrer AB. Bi-phasic growth patterns in rice. *Ann Bot* (Lond) 2004;94:811-7.
28. Fujikawa H, Morozumi S. Modeling surface growth of escherichia coli on agar plates. *Appl Environ Microbiol* 2005;71:7920-6.
29. Sakamoto T, Matsubara H, Hata Y, et al. Logistic character of myocardial twitch force curve: simulation. *Heart Vessel* 1996; 11:171-9.

APPENDIX

The following h-L function is used to curve-fit CaTI data by the least-squares method:

$$Ca(t) = 2Ca_{1A}/\{1 + \exp[-(t - t_{aC})/Ca\tau_{1L}]\} + Ca_{1B} \quad \text{(Eq. 3)}$$

where t is the time from the point corresponding to the beginning of twitch stimulation to the point corresponding to dCa/dt_{max}, Ca_{1A} is the h-L amplitude constant of CaTI, $Ca\tau_{1L}$ is the h-L time constant of CaTI, Ca_{1B} is the h-L non-zero asymptote of CaTI, and t_{aC} is a constant which represents the time at the point corresponding to dCa/dt_{max}.[2] It is noted that t_{aC} is determined before the h-L curve fitting. The h-L function curve given by Eq. 3 increases monotonically from Ca(0) (= Ca_{1B}) to $Ca(t_{aC})$ [= $(Ca_{1A} + Ca_{1B})$]. The $Ca\tau_{1L}$ value corresponds to the time duration for the curves to increase from $Ca(t_{aC} - Ca\tau_{1L})$ {= $[2Ca_{1A}/(1 + e) + Ca_{1B}]$~$(0.54\ Ca_{1A} + Ca_{1B})$} to $Ca(t_{aC})$ [= $(Ca_{1A} + Ca_{1B})$]. The Ca_{1A}, $Ca\tau_{1L}$, and Ca_{1B} values for the 15 isolated mouse LV papillary muscles were 869 ± 199 nmol/l, 2.22 ± 0.16 ms, and 1.50 ± 5.80 nmol/l, respectively.

The following m-E function is used to curve-fit CaTI data by the least-squares method:

$$Ca(t) = Ca_{10}\exp[(t - t_{aC})/Ca\tau_{1E}] + Ca_{1\infty} \quad \text{(Eq. 4)}$$

where t is the time from the point corresponding to twitch stimulation to the point corresponding to dCa/dt_{max}, Ca_{10} is the m-E amplitude constant of CaTI, $Ca\tau_{1E}$ is the m-E time constant of CaTI, $Ca_{1\infty}$ is the m-E non-zero asymptote of CaTI, and t_{aC} is a constant which represents the time at the point corresponding to dCa/dt_{max}. It is noted that t_{aC} is determined before the m-E curve fitting. The m-E function curve given by Eq. 4 increases monotonically from Ca(0) (= $Ca_{1\infty}$) to $Ca(t_{aC})$ [= $(Ca_{10} + Ca_{1\infty})$]. The $Ca\tau_{1E}$ value corresponds to the time duration for the curve to increase from $Ca(t_{aC} - Ca\tau_{1E})$ [= $(Ca_{10}/e + Ca_{1\infty})$~$(0.37Ca_{10} + Ca_{1\infty})$] to $Ca(t_{aC})$ [= $(Ca_{10} + Ca_{1\infty})$]. The Ca_{10}, $Ca\tau_{1E}$, and $Ca_{1\infty}$ values for the 15 isolated mouse LV papillary muscles were 899 ± 206 nmol/l, 3.08 ± 0.23 ms, and -0.25 ± 5.93 nmol/l, respectively.

The relationships between Ca_{1A} with Eq. 3 and the absolute value of Ca_{2A} with Eq. 1, and between Ca_{10} with Eq. 4 and the absolute value of Ca_{20} with Eq. 2 are shown in Figures 4A and B, respectively.

The relationships between $Ca\tau_{1L}$ with Eq. 3 and $Ca\tau_{2L}$ with Eq. 1, and between $Ca\tau_{1E}$ with Eq. 4 and $Ca\tau_{2E}$ with Eq. 2 are shown in Figures 5A and B, respectively.

The following h-L function is used to curve-fit CaTIV data by the least-squares method:

$$Ca(t) = 2Ca_{4A}/\{1 + \exp[(t - t_{dC})/Ca\tau_{4L}]\} + Ca_{4B} \quad \text{(Eq. 5)}$$

where t is the time from the point corresponding to twitch stimulation to the point corresponding to the resting Ca^{2+} concentration, Ca_{4A} is the h-L amplitude constant of CaTIV, $Ca\tau_{4L}$ is the h-L time constant of CaTIV, Ca_{4B} is the h-L non-zero asymptote of CaTIV, and t_{dC} is a constant which represents the time at the point corresponding to dCa/dt_{min}.[3] It is noted that t_{dC} is determined before the h-L curve fitting. The h-L function curve given by Eq. 5 decreases monotonically from $Ca(t_{dC})$ [= $(Ca_{4A} + Ca_{4B})$] to $Ca(\infty)$ [= Ca_{4B}]. The $Ca\tau_{4L}$ value corresponds to the time duration for the curves to decrease from $Ca(t_{dC})$ [= $(Ca_{4A} + Ca_{4B})$] to $Ca(t_{dC} + Ca\tau_{4L})$ {= $[2Ca_{4A}/(1 + e) + Ca_{4B}]$~$(0.54\ Ca_{4A} + Ca_{4B})$}. The Ca_{4A}, $Ca\tau_{4L}$, and Ca_{4B} values for the 15 isolated mouse LV papillary muscles were 1,252 ± 438 nmol/l, 38.04 ± 4.83 ms, and -0.59 ± 10.83 nmol/l, respectively.

The following m-E function is used to curve-fit CaTIV data by the least-squares method:

$$Ca(t) = Ca_{40}\exp[-(t - t_{dC})/Ca\tau_{4E}] + Ca_{4\infty} \quad \text{(Eq. 6)}$$

where t is the time from the point corresponding to twitch stimulation to the point corresponding to the resting Ca^{2+} concentration, Ca_{40} is the m-E amplitude constant of CaTIV, $Ca\tau_{4E}$ is the m-E time constant of CaTIV, $Ca_{4\infty}$ is the m-E non-zero asymptote of CaTIV, and t_{dC} is a constant which represents the time at the point corresponding to dCa/dt_{min}. It is noted that t_{dC} is determined before the m-E curve fitting. The m-E function curve given by Eq. 6 decreases monotonically from $Ca(t_{dC})$ [= $(Ca_{40} + Ca_{4\infty})$] to $Ca(\infty) = Ca_{4\infty}$. The $Ca\tau_{4E}$ value corresponds to the time duration for the curve to decrease from $Ca(t_{dC})$ [= $(Ca_{40} + Ca_{4\infty})$] to $Ca(t_{dC} + Ca\tau_{4E})$ [= $(Ca_{40}/e + Ca_{4\infty})$~$(0.37Ca_{40} + Ca_{4\infty})$]. The Ca_{40}, $Ca\tau_{4E,}$ and $Ca_{4\infty}$ values for the 15 isolated mouse LV papillary muscles were 1,347 ± 472 nmol/l, 52.2 ± 6.9 ms, and -12.06 ± 13.45 nmol/l, respectively.

The relationships between Ca_{4A} with Eq. 5 and the absolute value of Ca_{2A} with Eq. 1, and between Ca_{40} with Eq. 6 and the absolute value of Ca_{20} with Eq. 2 are shown in Figures 4C and D, respectively.

The relationships between $Ca\tau_{4L}$ with Eq. 5 and $Ca\tau_{2L}$ with Eq. 1, and between $Ca\tau_{4E}$ with Eq. 6 and $Ca\tau_{2E}$ with Eq. 2 are shown in Figures 5C and D, respectively.